

# From predictions to prescriptions: A data-driven response to COVID-19

Dimitris Bertsimas<sup>a,b,1</sup>, Leonard Boussoux<sup>b</sup>, Ryan Cory-Wright<sup>b</sup>, Arthur Delarue<sup>b</sup>, Vasileios Digalakis<sup>b</sup>, Alexandre Jacquillat<sup>a,b</sup>, Driss Lahlou Kitane<sup>b</sup>, Galit Lukin<sup>b</sup>, Michael Li<sup>b</sup>, Luca Mingardi<sup>b</sup>, Omid Nohadani<sup>c</sup>, Agni Orfanoudaki<sup>b</sup>, Theodore Papalexopoulos<sup>b</sup>, Ivan Paskov<sup>b</sup>, Jean Pauphilet<sup>b</sup>, Omar Skali Lami<sup>b</sup>, Bartolomeo Stellato<sup>b</sup>, Hamza Tazi Bouardi<sup>b</sup>, Kimberly Villalobos Carballo<sup>b</sup>, Holly Wiberg<sup>b</sup>, and Cynthia Zeng<sup>b</sup>

<sup>a</sup>Sloan School of Management, Massachusetts Institute of Technology, Cambridge, MA 02142; <sup>b</sup>Operations Research Center, Massachusetts Institute of Technology, Cambridge, MA 02139; <sup>c</sup>Benefits Science Technologies, Boston, MA 02110

This manuscript was compiled on May 26, 2020

1 The COVID-19 pandemic has created unprecedented challenges  
2 worldwide. Strained healthcare providers make difficult decisions  
3 on patient triage, treatment and care management on a daily basis.  
4 Policy makers have imposed social distancing measures to slow the  
5 disease, at a steep economic price. We design analytical tools to sup-  
6 port these decisions and combat the pandemic. Specifically, we pro-  
7 pose a comprehensive data-driven approach to understand the clin-  
8 ical characteristics of COVID-19, predict its mortality, forecast its evo-  
9 lution, and ultimately alleviate its impact. By leveraging cohort-level  
10 clinical data, patient-level hospital data, and census-level epidemi-  
11 ological data, we develop an integrated four-step approach, combin-  
12 ing descriptive, predictive and prescriptive analytics. First, we ag-  
13 gregate hundreds of clinical studies into the most comprehensive  
14 database on COVID-19 to paint a new macroscopic picture of the dis-  
15 ease. Second, we build personalized calculators to predict the risk  
16 of infection and mortality as a function of demographics, symptoms,  
17 comorbidities, and lab values. Third, we develop a novel epidemi-  
18 ological model to project the pandemic's spread and inform social  
19 distancing policies. Fourth, we propose an optimization model to re-  
20 allocate ventilators and alleviate shortages. Our results have been  
21 used at the clinical level by several hospitals to triage patients, guide  
22 care management, plan ICU capacity, and re-distribute ventilators. At  
23 the policy level, they are currently supporting safe back-to-work poli-  
24 cies at a major institution and equitable vaccine distribution planning  
25 at a major pharmaceutical company, and have been integrated into  
26 the US Center for Disease Control's pandemic forecast.

COVID-19 | Epidemiological modeling | Machine learning | Optimization

1 In just a few weeks, the whole world has been upended by the  
2 outbreak of COVID-19, an acute respiratory disease caused  
3 by a new coronavirus called SARS-CoV-2. The virus is highly  
4 contagious: it is easily transmitted from person to person via  
5 respiratory droplet nuclei and can persist on surfaces for days  
6 (1, 2). As a result, COVID-19 has spread rapidly—classified by  
7 the World Health Organization as a public health emergency  
8 on January 30, 2020 and as a pandemic on March 11. As of  
9 mid-May, over 4.5 million cases and 300,000 deaths have been  
10 reported globally (3).

11 Because no treatment is currently available, healthcare  
12 providers and policy makers are wrestling with unprecedented  
13 challenges. Hospitals and other care facilities are facing short-  
14 ages of beds, ventilators and personal protective equipment—  
15 raising hard questions on how to treat COVID-19 patients  
16 with scarce supplies and how to allocate resources to prevent  
17 further shortages. At the policy level, most countries have  
18 imposed “social distancing” measures to slow the spread of the  
19 pandemic. These measures allow strained healthcare systems

to cope with the disease by “flattening the curve” (4) but  
also come at a steep economic price (5, 6). Nearly all govern-  
ments are now confronted to difficult decisions balancing  
public health and socio-economic outcomes.

This paper proposes a comprehensive data-driven approach  
to understand the clinical characteristics of COVID-19, predict  
its mortality, forecast its evolution, and ultimately alleviate  
its impact. We leverage a broad range of data sources, which  
include (i) our own cohort-level data aggregating hundreds of  
clinical studies, (ii) patient-level data obtained from electronic  
health records, and (iii) census reports on the scale of the pan-  
demic. We develop an integrated approach spanning descrip-  
tive analytics (to derive a macroscopic understanding of the  
disease), predictive analytics (to forecast the near-term impact  
and longer-term dynamics of the pandemic), and prescriptive  
analytics (to support healthcare and policy decision-making).

Specifically, our approach comprises four steps (Figure 1):

- *Aggregating and visualizing the most comprehensive clin-  
ical database on COVID-19 (Section 1).* We aggregate  
cohort-level data on demographics, comorbidities, symp-  
toms and lab values from 160 clinical studies. These data  
paint a broad picture of the disease, identifying common  
symptoms, disparities between mild and severe patients,

## Significance Statement

In the midst of the COVID-19 pandemic, healthcare providers  
and policy makers are wrestling with unprecedented challenges.  
How to treat COVID-19 patients with equipment shortages?  
How to allocate resources to combat the disease? How to plan  
for the next stages of the pandemic? We present a data-driven  
approach to tackle these challenges. We gather comprehensive  
data from various sources, including clinical studies, electronic  
medical records, and census reports. We develop algorithms to  
understand the disease, predict its mortality, forecast its spread,  
inform social distancing policies, and re-distribute critical equip-  
ment. These algorithms provide decision support tools that  
have been deployed on our publicly available website, and  
are actively used by hospitals, companies, and policy makers  
around the globe.

D.B., R.C.W., A.D., A.J., D.L.K., M.L., O.N., A.O., I.P., J.P., O.S.L., B.S., H.T.B. and H.W. designed  
research; L.B., R.C.W., A.D., V.D., A.J., D.L.K., G.L., M.L., L.M., A.O., T.P., I.P., J.P., O.S.L., B.S.,  
H.T.B., K.V.C., H.W. and C.Z. performed research; R.C.W., A.D., D.L.K., M.L., L.M., A.O., T.P., I.P.,  
J.P., O.S.L., B.S., H.T.B., and H.W. analyzed data; D.B., R.C.W., A.D., A.J., M.L., O.N., A.O., J.P.,  
H.T.B. and H.W. wrote the paper.

No author has any competing interest to declare.

<sup>1</sup>To whom correspondence should be addressed. E-mail: dbertsim@mit.edu

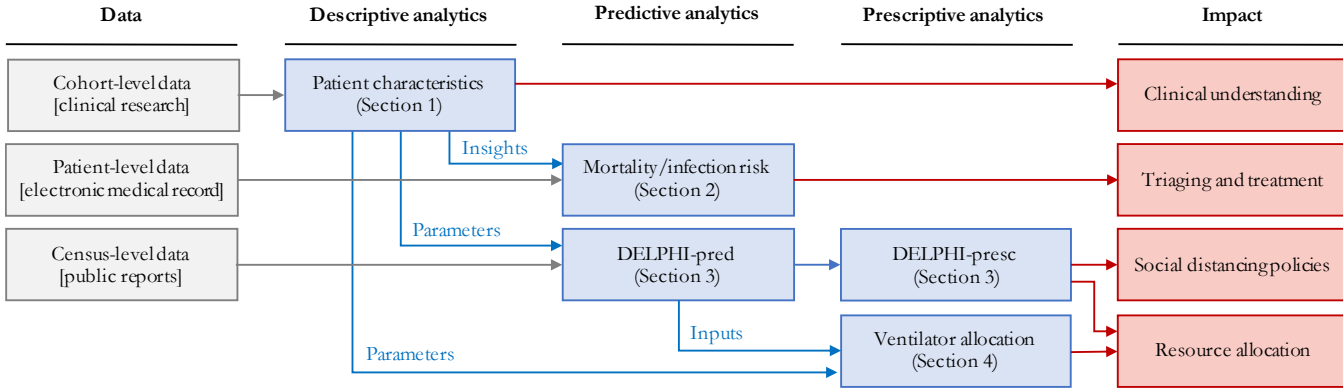


**Fig. 1.** Overview of our end-to-end analytics approach. We leverage diverse data sources to inform a family of descriptive, predictive and prescriptive tools for clinical and policy decision-making support.

and geographic disparities—insights that are hard to derive from any single study and can orient future clinical research on COVID-19, its mutations, and its disparate effects across ethnic groups.

- *Providing personalized indicators to assess the risk of mortality and infection (Section 2).* Using patient-level data, we develop machine learning models to predict mortality and infection risk, as a function of demographics, symptoms, comorbidities, and lab values. Using gradient boosting methods, the models achieve strong predictive performance—with an out-of-sample area under the curve above 90%. These models yield personalized calculators that can (i) guide triage, treatment, and care management decisions for strained healthcare systems, and (ii) serve as pre-screening tools for patients before they visit healthcare or testing facilities.
- *Developing a novel epidemiological model to forecast the evolution of the disease and assess the effects of social distancing (Section 3).* We propose a new compartmental model called DELPHI, which accounts for COVID-19 features such as underdetection and government response. The model estimates the disease’s spread with high accuracy; notably, its projections from as early as April 3 have matched the number of cases observed in the United States up to mid-May. We also provide a data-driven assessment of social distancing policies, showing that the pandemic’s spread is highly sensitive to the stringency and timing of mitigating measures.
- *Proposing an optimization model to support ventilator allocation in response to the pandemic (Section 4).* We formulate a mixed-integer optimization model to allocate ventilators efficiently in a semi-collaborative setting where resources can be shared both between healthcare facilities or through a central authority. In the United States, this allows us to study the trade-offs of managing the federal ventilator stockpile in conjunction with inter-state transfers. Results show that limited ventilator transfers could have eliminated shortages in April 2020.

A major contribution of our work is to treat these different questions as interdependent challenges raised by the pandemic—as opposed to a series of isolated problems. Indeed, clinical decision-making depends directly on patient inflows and available supplies, while resource planning and govern-

ment responses react to patient-level outcomes. By combining various data sources into descriptive, predictive and prescriptive methods, this paper proposes an end-to-end approach to design a comprehensive and cohesive response to COVID-19.

Ultimately, this paper develops analytical tools to inform clinical and policy responses to the COVID-19 pandemic. These tools are available to the public on a dedicated website.\* They have also been deployed in practice to combat the spread of COVID-19 globally. Several hospitals in Europe have used our risk calculators to support pre-triage and post-triage decisions, and a major financial institution in South America is applying our infection risk calculator to determine how employees can safely return to work. A major hospital system in the United States planned its intensive care unit (ICU) capacity based on our forecasts, and leveraged our optimization results to allocate ventilators across hospitals when the number of cases was rising. Our epidemiological predictions are used by a major pharmaceutical company to design a vaccine distribution strategy that can contain future phases of the pandemic. They have also been incorporated into the US Center for Disease Control’s forecasts (7).

## 1. Descriptive Analytics: Clinical Outcomes Database

Early responses to the COVID-19 pandemic have been inhibited by the lack of available data on patient outcomes. Individual centers released reports summarizing patient characteristics. Yet, this decentralized effort makes it difficult to construct a cohesive picture of the pandemic.

To address this problem, we construct a database that aggregates demographics, comorbidities, symptoms, laboratory blood test results (“lab values”, henceforth) and clinical outcomes from 160 clinical studies released between December 2019 and May 2020—made available on our website for broader use. The database contains information on 133,600 COVID-19 patients (3.13% of the global COVID-19 patients as of May 12, 2020), spanning mainly Europe (81,207 patients), Asia (19,418 patients) and North America (23,279 patients). To our knowledge, this is the largest dataset on COVID-19.

**A. Data Aggregation.** Each study was read by an MIT researcher, who transcribed numerical data from the manuscript. The appendix reports the main transcription assumptions.

\* [www.covidanalytics.io](http://www.covidanalytics.io)

126 Each row in the database corresponds to a cohort of  
127 patients—some papers study a single cohort, whereas others  
128 study several cohorts or sub-cohorts. Each column reports  
129 cohort-level statistics on demographics (e.g., average age, gender  
130 breakdown), comorbidities (e.g., prevalence of diabetes,  
131 hypertension), symptoms (e.g., prevalence of fever, cough),  
132 treatments (e.g., prevalence of antibiotics, intubation), lab  
133 values (e.g., average lymphocyte count), and clinical outcomes  
134 (e.g., average hospital length of stay, mortality rate). We also  
135 track whether the cohort comprises “mild” or “severe” patients  
136 (mild and severe cohorts are only a subset of the data).

137 Due to the pandemic’s urgency, many papers were published  
138 before all patients in a cohort were discharged or deceased. Accord-  
139 ingly, we estimate the mortality rate from discharged and  
140 deceased patients only (referred to as “Projected Mortality”).

141 **B. Objectives.** Our main goal is to leverage this database to  
142 derive a macroscopic understanding of the disease. We break  
143 it down into the following questions:

- 144 • Which symptoms are most prevalent?
- 145 • How do “mild” and “severe” patients differ in terms of  
146 symptoms, comorbidities, and lab values?
- 147 • Can we identify epidemiological differences in different  
148 parts of the world?

149 **C. Descriptive Statistics.** Table 1 depicts the prevalence of  
150 COVID-19 symptoms, in aggregate, classified into “mild” or  
151 “severe” patients, and classified per geographic region. Our  
152 key observations are that:

- 153 • Cough, fever, shortness of breath, and fatigue are the  
154 most prevalent symptoms of COVID-19.
- 155 • COVID-19 symptoms are much more diverse than those  
156 listed by public health agencies. COVID-19 patients can  
157 experience at least 15 different symptoms. In contrast,  
158 the US Center for Disease Control and Prevention lists  
159 seven symptoms (cough, shortness of breath, fever, chills,  
160 myalgia, sore throat, and loss of taste/smell) (8); the  
161 World Health Organization lists three symptoms (fever,  
162 cough, and fatigue) (9); and the UK National Health  
163 Service lists two main symptoms (fever and cough) (10).  
164 This suggests a lack of consensus among the medical  
165 community, and opportunities to revisit public health  
166 guidelines to capture the breadth of observed symptoms.
- 167 • Shortness of breath and elevated respiratory rates are  
168 much more prevalent in cases diagnosed as severe.
- 169 • Symptoms are quite different in Asia vs. Europe or North  
170 America. In particular, more than 75% of Asian patients  
171 experience fever, as compared to less than half in Europe  
172 and North America. Alternatively, shortness of breath is  
173 much more prevalent in Europe and North America.

174 Using a similar nomenclature, Figure 2A reports demo-  
175 graphics, comorbidities, lab values, and clinical outcomes (an  
176 extended version is available in the appendix). In terms of  
177 demographics, severe populations of patients have a higher  
178 incidence of male subjects and are older on average. Severe  
179 patients also have elevated comorbidity rates. Figures 2B  
180 and 2C visually confirm the impact of age and hypertension  
181 rates on population-level mortality—consistently with (11–13).  
182 In terms of lab values, CRP, AST, BUN, IL-6 and Protocalci-  
183 tonin are highly elevated among severe patients.

184 **D. Discussion and Impact.** Our database is the largest avail-  
185 able source of clinical information on COVID-19 assembled  
186 to date. As such, it provides new insights on common symp-  
187 toms and the drivers of the disease’s severity. Ultimately, this  
188 database can support guidelines from health organizations,  
189 and contribute to ongoing clinical research on the disease.

190 Another benefit of this database is its geographical reach.  
191 Results highlight disparities in patients’ symptoms across  
192 regions. These disparities may stem from (i) different reporting  
193 criteria; (ii) different treatments; (iii) disparate impacts across  
194 different ethnic groups; and (iv) mutations of the virus since  
195 it first appeared in China. This information contributes to  
196 early evidence on COVID-19 mutations (14, 15) and on its  
197 disparate effects on different ethnic groups (16, 17).

198 Finally, the database provides average values of key param-  
199 eters into our epidemiological model of the disease’s spread  
200 and our optimization model of resource allocation (e.g., av-  
201 erage length of stay of hospitalizations, average fraction of  
202 hospitalized patients put on a ventilator).

203 The insights derived from this descriptive analysis highlight  
204 the need for personalized data-driven clinical indicators. Yet,  
205 our population-level database cannot be leveraged directly  
206 to support decision-making at the patient level. We have  
207 therefore initiated a multi-institution collaboration to collect  
208 electronic medical records from COVID-19 patients and de-  
209 velop clinical risk calculators. These calculators, presented in  
210 the next section, are informed by several of our descriptive  
211 insights. Notably, the disparities between severe patients and  
212 the rest of the patient population inform the choice of the fea-  
213 tures included in our mortality risk calculator. Moreover, the  
214 geographic disparities suggest that data from Asia may be less  
215 predictive when building infection or mortality risk calculators  
216 designed for patients in Europe or North America—motivating  
217 our use of data from Europe.

## 2. Predictive Analytics: Mortality and Infection Risk

218 Throughout the COVID-19 crisis, physicians have made dif-  
219 ficult triage and care management decisions on a daily basis.  
220 Oftentimes, these decisions could only rely on small-scale  
221 clinical tests, each requiring significant time, personnel and  
222 equipment and thus cannot be easily replicated. Once the  
223 burden on “hot spots” has ebbed, hospitals began to aggregate  
224 rich data on COVID-19 patients. This data offers opportuni-  
225 ties to develop algorithmic risk calculators for large-scale  
226 decision support—ultimately facilitating a more proactive and  
227 data-driven strategy to combat the disease globally.

228 We have established a patient-level database of thousands of  
229 COVID-19 hospital admissions. Using state-of-the-art machine  
230 learning methods, we develop a *mortality risk calculator* and an  
231 *infection risk calculator*. Together, these two risk assessments  
232 provide screening tools to support critical care management  
233 decisions, spanning patient triage, hospital admissions, bed  
234 assignment and testing prioritization.

235 **A. Methods.** This investigation constitutes a multi-center  
236 study from healthcare institutions in Spain and Italy, two  
237 countries severely impacted by COVID-19. Specifically, we  
238 collected data from (i) Azienda Socio-Sanitaria Territoriale  
239 di Cremona (ASST Cremona), the main hospital network in  
240 the Province of Cremona, and (ii) HM Hospitals, a leading  
241 hospital group in Spain with 15 general hospitals and 21 clin-  
242 ical

**Table 1. Count and prevalence of symptoms among COVID-19 patients, in aggregate, broken down into mild/severe patients, and broken down per continent (Asia, Europe, North America). Mild and severe patients only form a subset of the data, and so do patients from Asia, Europe and North America. A “-” indicates that fewer than 100 patients in a subpopulation reported on this symptom.**

Symptom	All patients		Mild		Severe		Asia		Europe		North America	
	Count	(%)	Count	(%)	Count	(%)	Count	(%)	Count	(%)	Count	(%)
Cough	94,950	52.8%	6,833	63.0%	5,803	50.4%	14,034	56.2%	78,430	52.2%	1,113	63.6%
Fever	95,870	48.1%	6,864	79.3%	6,077	76.7%	14,750	76.6%	78,450	43.5%	1,481	41.3%
Short Breath	17,290	33.7%	6,006	16.1%	5,373	60.7%	11,330	19.7%	3,512	69.9%	1,111	49.2%
Fatigue	11,560	31.4%	5,313	35.3%	1,989	40.6%	11,320	30.8%	226	64.2%	—	—
Sputum	7,613	26.3%	4,995	29.2%	1,216	34.2%	7,395	26.7%	—	—	176	10.9%
Sore Throat	83,170	22.2%	3,513	14.2%	921	8.2%	6,013	10.4%	75,235	22.9%	550	9.8%
Myalgia	12,150	17.5%	4,455	16.4%	1,643	19.1%	8,517	15.5%	1,633	33.5%	755	25.3%
Elev. Resp. Rate	7,376	16.4%	527	9.7%	642	38.4%	1,257	14.6%	—	—	6,117	16.8%
Anorexia	3,928	15.8%	1,641	14.2%	808	15.4%	3,566	13.8%	312	40.5%	—	—
Headache	11,430	15.7%	5,068	12.2%	1,541	8.6%	7,929	9.9%	1,633	27.2%	551	8.7%
Nausea	10,070	12.4%	4,238	6.5%	1,798	5.6%	8,262	8.2%	312	22.4%	259	9.0%
Chest Pain	3,303	11.3%	767	12.2%	588	19.6%	2,984	12.2%	—	—	—	—
Diarrhea	16,520	11.1%	5,687	9.7%	5,369	9.0%	11,470	10.8%	3,512	10.4%	1,066	15.4%
Cong. Airway	1,639	8.7%	2,176	6.5%	234	14.1%	1,369	8.9%	—	—	258	7.4%
Chills	3,116	8.7%	2,751	9.9%	520	9.4%	2,794	8.2%	—	—	268	11.5%
Proj. Mortality	111,700	11.7%	7,428	0.4%	9,146	74.0%	12,820	16.7%	79,750	9.9%	19,060	15.8%

Feature	All	Mild	Severe
<b>Demographics</b>			
Male (%)	53.0%	48.8%	68.7%
Age (years)	51.3	46.1	68.2
White/European (%)	22.2%	9.7%	63.9%
African American (%)	5.4%	3.5%	2.5%
Asian (%)	51.3%	80.2%	31.2%
Hispanic/Latino	19.9%	0%	0%
Multiple ethnicities/other	3.6%	6.9%	2.7%
<b>Comorbidities</b>			
Smoking history	16.1%	12.2%	16.6%
Hypertension	35.9%	15.2%	54.4%
Diabetes	20.8%	6.8%	26.1%
Cardio Disease	12.4%	3.0%	20.3%
COPD	6.0%	2.8%	10.0%
Cancer	7.2%	3.2%	12.9%
Liver Disease	2.8%	2.3%	3.5%
Cerebrovascular	9.8%	2.7%	24.8%
Kidney Disease	5.7%	1.2%	10.8%
<b>Lab values</b>			
White Blood Cells Count (WBC) ( $10^9/L$ )	6.41	5.07	6.80
Neutrophil Count ( $10^9/L$ )	4.72	5.12	5.78
Platelet Count ( $10^9/L$ )	195.7	184.0	170.4
Alanine Aminotransferase (ALT) (U/L)	29.0	24.6	31.1
Aspartate Aminotransferase (AST) (U/L)	37.3	27.1	45.7
Blood Urea Nitrogen Count (BUN) (mmol/L)	5.22	4.18	6.86
Creatinine ( $\mu\text{mol}/L$ )	63.08	66.0	56.4
C-Reactive Protein Count (CRP) (mg/L)	76.5	18.9	94.1
Interleukin-6 (IL-6) (pg/mL)	24.57	4.17	38.63
Procalcitonin (ng/mL)	2.26	1.85	4.81
Length of Stay (days)	10.7	14.0	7.97

A

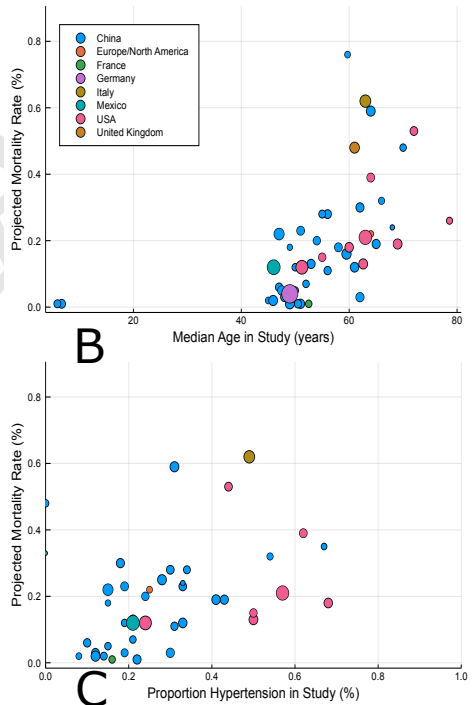


**Fig. 2.** Summary of demographics, comorbidities and lab values in mild and severe COVID-19 patients. (A) Comorbidities, demographics, average lab values, average length of stay and projected mortality among COVID-19 patients, in aggregate and broken down into mild/severe patients. (B) Impact of median age on projected mortality at a cohort level. (C) Impact of hypertension rates on projected mortality at a cohort level. The size of each dot represents the number of patients in the cohort, and its color represents the nation the study was performed in. We only include studies reporting both discharged and deceased patients.

cal centers spanning the regions of Madrid, Galicia, and León. We applied the following inclusion criteria to the calculators:

- **Mortality Risk:** We include adult patients diagnosed with COVID-19 and hospitalized. We consider patients who were either discharged from the hospital or deceased within the visit—excluding active patients. We include

only lab values and vital values collected on the first day in the emergency department to match the clinical decision setting—predicting prognosis at the time of admission.

- **Infection Risk:** We include adult patients who underwent a polymerase chain reaction test for detecting

254 COVID-19 infection at the ASST Cremona hospital (18).<sup>†</sup>  
255 We include all patients, regardless of their clinical outcome.  
256 Each patient was subject to a blood test. We omit comorbidities since they are derived from the discharge  
257 diagnoses, hence not available for all patients.  
258

259 We train two models for each calculator: one with lab  
260 values and one without lab values. Missing values are imputed  
261 using  $k$ -nearest neighbors imputation (19). We exclude  
262 features missing for more than 40% of patients. We train  
263 binary classification models for both risk calculators, using the  
264 XGBoost algorithm (20). We restrict the model to select at  
265 most 20 features, in order to make the resulting tool easily us-  
266 able. We use SHapley Additive exPlanations (SHAP) (21, 22)  
267 to generate importance plots that identify risk drivers and  
268 provide transparency on the model predictions.

269 To evaluate predictive performance, we use 40 random data  
270 partitions into training and test sets. We compute the average  
271 Area Under the Curve (AUC), sensitivity, specificity, precision,  
272 negative predictive value, and positive predictive value. We  
273 calculate 95% confidence intervals using bootstrapping.

## 274 **B. Results.**

275 **Study Population.** The mortality study population comprises  
276 2,831 patients, 711 (25.1%) of whom died during hospitaliza-  
277 tion while the remaining ones were discharged. The infection  
278 study population comprises 3,135 patients, 1,661 (53.0%) of  
279 whom tested positive for COVID-19. The full distributions of  
280 patient characteristics are reported in the appendix.

281 **Performance Evaluation.** All models achieve strong out-of-sample  
282 performance. Our mortality risk calculator has an AUC of  
283 93.8% with lab values and 90.5% without lab values. Our  
284 infection risk calculator has an AUC of 91.8% with lab values  
285 and 83.1% without lab values. These values suggest a strong  
286 discriminative ability of the proposed models. We report in  
287 the appendix average results across all random data partitions.

288 We also report in the appendix threshold-based metrics,  
289 which evaluate the discriminative ability of the calculators  
290 at a fixed cutoff. Using cutoff to ensure a sensitivity of at  
291 least 90% (motivated by the high costs of false negatives), we  
292 obtain an accuracy spanning 65%–80%.

293 The mortality model achieves better overall predictive per-  
294 formance than the infection model. As expected, both models  
295 have better predictive performance with lab values than with-  
296 out lab values. Yet, the models without lab values still achieve  
297 strong predictive performance.

298 **Model Interpretation.** Figure 3 plots the SHAP importance plots  
299 for all models. The figures sort the features by decreasing  
300 significance. For each one, the row represents its impact on  
301 the SHAP value, as the feature ranges from low (blue) to high  
302 (red). Higher SHAP values correspond to increased likelihood  
303 of a positive outcome (i.e. mortality or infection). Features  
304 with the color scale oriented blue to red (resp. red to blue)  
305 from left to right have increasing (resp. decreasing) risk as the  
306 feature increases. For example, “Age” is the most important  
307 feature of the mortality score with lab values (Figure 3A), and  
308 older patients have higher predicted mortality.

† HM Hospitals patients were not included since no negative case data was available.

309 **C. Discussion and Impact.** The models with lab values provide  
310 algorithmic screening tools that can deliver COVID-19 risk  
311 predictions using common clinical features. In a constrained  
312 healthcare system or in a clinic without access to advanced  
313 diagnostics, clinicians can use these models to rapidly identify  
314 high-risk patients to support triage and treatment decisions.

315 The models without lab values offer an even simpler tool  
316 that could be used outside of a clinical setting. In strained  
317 healthcare systems, it can be difficult for patients to obtain  
318 direct advice from providers. Our tool could serve as a pre-  
319 screening step to identify personalized infection risk—without  
320 visiting a testing facility. While the exclusion of lab values  
321 reduces the AUC (especially for infection), these calculators  
322 still achieve strong predictive performance.

323 Our models provide insights into risk factors and biomark-  
324 ers related to COVID-19 infection and mortality. Our results  
325 suggest that the main indicators of mortality risk are age,  
326 BUN, CRP, AST, and low oxygen saturation. These findings  
327 validate several population-level insights from Section 1 and  
328 are in agreement with clinical studies: prevalence of shortness  
329 of breath (23), elevated levels of CRP as an inflammatory  
330 marker (24, 25), and elevated AST levels due to liver dysfunc-  
331 tion in severe COVID-19 cases (11, 26).

332 Turning to infection risk, the main indicators are CRP,  
333 Leukocytes, Calcium, AST, and temperature. These findings  
334 are also in agreement with clinical reports: an elevated CRP  
335 generally indicates an early sign of infection and implies lung  
336 lesions from COVID-19 (27), elevated levels of leukocytes  
337 suggest cytokine release syndrome caused by SARS-CoV-2  
338 virus (28), and lowered levels of serum calcium signal higher  
339 rate of organ injury and septic shock (29). Since our findings  
340 agree with clinical observations, our calculators can be used  
341 to support clinical decision making—although they are not  
342 intended to substitute clinical diagnostic or medical expertise.

343 When lab values are not available, the widely accepted  
344 risk factors of age, oxygen saturation, temperature, and heart  
345 rate become the key indicators for both risk calculators. We  
346 observe that mortality risk is higher for male patients (blue in  
347 Figure 3B) than for female patients (red), confirming clinical  
348 reports (30, 31). An elevated respiratory frequency becomes  
349 an important predictor of infection, as reported in (32). These  
350 findings suggest that demographics and vitals provide valuable  
351 information in the absence of lab values. However, when lab  
352 values are available, these other features become secondary.

353 A limitation of the current mortality model is that it does  
354 not take into account medication and treatments during hos-  
355 pitalization. We intend to incorporate these in future research  
356 to make these models more actionable. Furthermore, these  
357 models aim to reveal associations between risks and patient  
358 characteristics but are not designed to establish causality.

359 Overall, we have developed data-driven calculators that  
360 allow physicians and patients to assess mortality and infection  
361 risks in order to guide care management—especially with  
362 scarce healthcare resources. These calculators are being used  
363 by several hospitals within the ASST Cremona system to  
364 support triage and treatment decisions—alleviating the toll of  
365 the pandemic. Our infection calculator also supports safety  
366 protocols for Banco de Credito del Peru, the largest bank in  
367 Peru, to determine how employees can return to work.

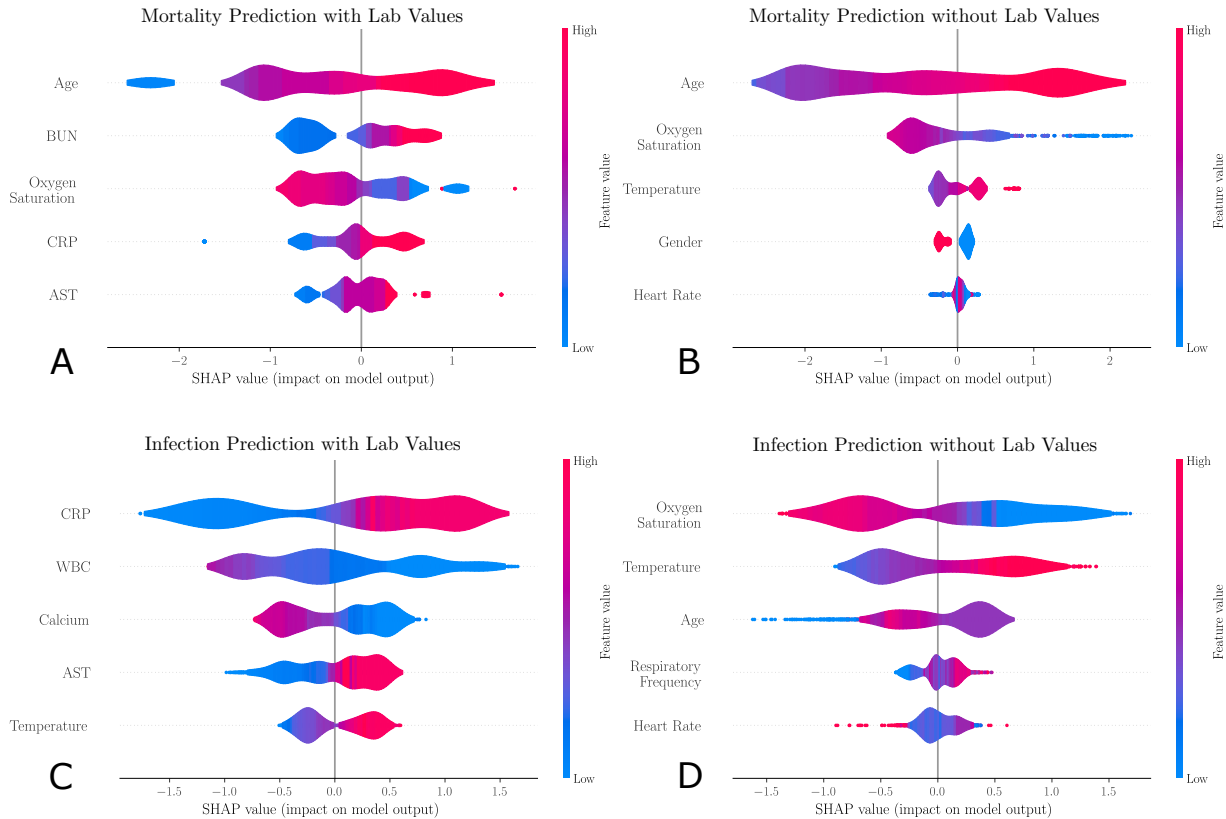


**Fig. 3.** SHapley Additive exPlanations (SHAP) importance plots for the mortality and infection risk calculators, including: (A) the mortality model with lab values; (B) the mortality model without lab values; (C) the infection model with lab values; and (D) the infection model without lab values. The five most important features are shown for each model. Gender is a binary feature (female is equal to 1, shown in red; male is equal to 0, shown in blue). Each row represents the impact of a feature on the outcome, with higher SHAP values indicating higher likelihood of a positive outcome.

### 368    3. Predictive and Prescriptive Analytics: Disease Pro- 369    jections and Government Response

370    We develop a new epidemiological model, called DELPHI  
371    (Differential Equations Leads to Predictions of Hospitalizations  
372    and Infections). The model first provides a predictive tool to  
373    forecast the number of detected cases, hospitalizations and  
374    deaths—we refer to this model as “DELPHI-pred”. It then  
375    provides a prescriptive tool to simulate the effect of policy  
376    interventions and guide government response to the COVID-19  
377    pandemic—we refer to this model as “DELPHI-presc”. All  
378    models are fit in each US state (plus the District of Columbia).

#### 379    A. DELPHI-pred: Projecting Early Spread of COVID-19.

380    **A.1. Model Development.** DELPHI is a compartmental model,  
381    with dynamics governed by ordinary differential equations.  
382    It extends the standard SEIR model by defining 11 states  
383    (Figure 4A): susceptible ( $S$ ), exposed ( $E$ ), infectious ( $I$ ), unde-  
384    tected people who will recover ( $U_R$ ) or decease ( $U_D$ ), detected  
385    hospitalized people who will recover ( $DH_R$ ) or decease ( $DH_D$ ),  
386    quarantined people who will recover ( $DQ_R$ ) or decease ( $DQ_D$ ),  
387    recovered ( $R$ ) and deceased ( $D$ ). The separation of the  $U_R/U_D$ ,  
388     $DQ_R/DQ_D$  and  $DH_R/DH_D$  states enables separate fitting of  
389    recoveries and deaths from the data.

390    As opposed to other COVID-19 models (see, e.g., 33), DEL-  
391    PHI captures two key elements of the pandemic:

- **Underdetection:** Many cases remain undetected due to limited testing, record failures, and detection errors. Ignoring them would underestimate the scale of the pandemic. We capture them through the  $U_R$  and  $U_D$  states. 392
- **Government Response:** “Social distancing” policies 393 limit the spread of the virus. Ignoring them would over- 394 estimate the spread of the pandemic. We model them 395 through a decline in the infection rate over time. Specifically, we write:  $\frac{dS}{dt} = -\alpha\gamma(t)S(t)I(t)$ , where  $\alpha$  is a 396 constant baseline rate and  $\gamma(t)$  is a time-dependent function 397 characterizing each state’s policies, modeled as follows: 398

$$\gamma(t) = \frac{2}{\pi} \arctan\left(\frac{-(t-t_0)}{k}\right) + 1. \quad 403$$

The inverse tangent function provides a concave-convex relationship, capturing three phases of government response. In *Phase I*, most activities continue normally as people adjust their behavior. In *Phase II*, the infection rate declines sharply as policies are implemented. In *Phase III*, the decline in the infection rate reaches saturation. The parameters  $t_0$  and  $k$  can be respectively thought of as the start date and the strength of the response. 404

405    Ultimately, DELPHI involves 13 parameters that define 406 the transition rates between the 11 states. We calibrate six of 407 them from our clinical outcomes database (Section 1). Using 408

415 non-linear optimization, we estimate seven parameters for each  
416 US state from the data to minimize in-sample error. This  
417 training procedure leverages historical data on the number of  
418 cases and deaths per US county (34). We include each state  
419 as soon as it records more than 100 cases. We provide details  
420 on the fitting procedure in the appendix.

421 **A.2. Validation.** DELPHI was created in late March and has been  
422 continuously updated to reflect new observed data. Figure 4B  
423 shows our projections made on three different dates, and  
424 compares them against historical observations. This plot  
425 focuses on the number of cases, but a similar plot for the  
426 number of deaths is reported in the appendix.

427 In addition to providing aggregate validation figures, we  
428 also evaluate the model's out-of-sample performance quanti-  
429 tatively, using a backtesting procedure. To our knowledge,  
430 this represents the first attempt to assess the predictive per-  
431 formance of COVID-19 projections. Specifically, we fit the  
432 model's parameters using data up to April 27, build projec-  
433 tions from April 28 to May 12, and evaluate the resulting  
434 Mean Absolute Percentage Error (MAPE). Figure 4C reports  
435 the results in each US state.

436 **A.3. Discussion and Impact.** Results suggest that DELPHI-pred  
437 achieves strong predictive performance. The model has been  
438 consistently predicting, with high accuracy the overall spread  
439 of the disease for several weeks. Notably, DELPHI-pred was  
440 able to anticipate, as early as April 3rd, the dynamics of the  
441 pandemic in the United States up to mid-May. At a time  
442 where 200,000–300,000 cases were reported, the model was  
443 predicting 1.2M–1.4M cases by mid-May—a prediction that  
444 became accurate 40 days later.

445 Our quantitative results confirm the visual evidence. The  
446 MAPE is small across US states. The median MAPE is 8.5%  
447 for the number of cases—the 10% and 90% percentiles are  
448 equal to 1.9% and 16.7%. The median MAPE is 7.8% for the  
449 number of deaths—the 10% and 90% percentiles are equal  
450 to 3.3% and 25.1%. Given the high level of uncertainty and  
451 variability in the disease's spread, this level of accuracy is  
452 suggestive of excellent out-of-sample performance.

453 As Figure 4C shows, a limitation of our model is that  
454 the relative error remains large for a small minority of US  
455 states. These discrepancies stem from two main reasons. First,  
456 errors are typically larger for states that have recorded few  
457 cases (WY) or few deaths (AK, KS, NE). Like all SEIR-  
458 derived models, DELPHI performs better on large populations.  
459 Moreover, the MAPE metric emphasizes errors on smaller  
460 population counts. Second, our model is fitted at the state  
461 level, implicitly assuming that the spread of the pandemic is  
462 independent from one state to another—thus ignoring inter-  
463 state travel. This limitation helps explain the above-median  
464 error in a few heartland states which were confronted to the  
465 pandemic in later stages (MN, TN, IA).

466 In summary, DELPHI-pred is a novel epidemiological model  
467 of the pandemic, which provides high-quality estimates of  
468 the daily number of cases and deaths per US state. This  
469 model has been incorporated to the forecasts used by the US  
470 Center for Disease Control to chart and anticipate the spread  
471 of the pandemic (7). It has also been used by the Hartford  
472 HealthCare system—the major hospital system in Connecticut,  
473 US—to plan its ICU capacity, and by a major pharmaceutical  
474 company to design a vaccine distribution strategy that can

most effectively contain the next phases of the pandemic.

475  
476 **B. DELPHI-presc: Toward Re-opening Society.** To inform the  
477 relaxation of social distancing policies, we link policies to the  
478 infection rate using machine learning. Specifically, we predict  
479 the values of  $\gamma(t)$ , obtained from the fitting procedure of  
480 DELPHI-pred. For simplicity and interpretability, we consider  
481 a simple model based on regression trees (35) and restrict the  
482 independent variables to the policies in place. We classify  
483 policies based on whether they restrict mass gatherings, school  
484 and/or other activities (referred to as “Others”, and including  
485 business closures, severe travel limitations and/or closing of  
486 non-essential services). We define a set of seven mutually  
487 exclusive and collectively exhaustive policies observed in the  
488 US data: (i) *No measure*; (ii) *Restrict mass gatherings*; (iii)  
489 *Restrict others*; (iv) *Authorize schools, restrict mass gatherings*  
490 and *others*; (v) *Restrict mass gatherings and schools*; (vi)  
491 *Restrict mass gatherings, schools and others*; and (vii) *Stay-*  
492 *at-home*.

493 We report the regression tree in the appendix, obtained  
494 from state-level data in the United States. This model achieves  
495 an out-of-sample  $R^2$  of 0.8, suggesting a good fit to the data.  
496 As expected, more stringent policies lead to lower values of  
497  $\gamma(t)$ . The results also provide comparisons between various  
498 policies—for instance, school closures seem to induce a stronger  
499 reduction in the infection rate than restricting “other” activi-  
500 ties. More importantly, the model quantifies the impact of  
501 each policy on the infection rate. We then use these results  
502 to predict the value of  $\gamma(t)$  as a function of the policies (see  
503 appendix for details), and simulate the spread of the disease  
504 as states progressively loosen social distancing policies.

505 Figure 4D plots the projected case count in the State of New  
506 York (NY), for different policies (we report a similar plot for  
507 the death count in the appendix). Note that the stringency of  
508 the policies has a significant impact on the pandemic's spread  
509 and ultimate toll. For instance, relaxing all social distancing  
510 policies on May 12 can increase the *cumulative* number of  
511 cases in NY by up to 25% by September.

512 Using a similar nomenclature, Figure 4E shows the case  
513 count if all social distancing policies are relaxed on May 12 vs.  
514 May 26. Note that the timing of the policies also has a strong  
515 impact: a two-week delay in re-opening society can greatly  
516 reduce a resurgence in NY.

517 The road back to a new normal is not straightforward:  
518 results suggest that the disease's spread is highly sensitive to  
519 both the intensity and the timing of social distancing policies.  
520 As governments grapple with an evolving pandemic, DELPHI-  
521 presc can be a useful tool to explore alternative scenarios and  
522 ensure that critical decisions are supported with data.

#### 4. Prescriptive Analytics: Ventilator Allocation

523 COVID-19 is primarily an acute respiratory disease. The  
524 World Health Organization recommends that patients with  
525 oxygen saturation levels below 93% receive respiratory sup-  
526 port (9). Following the standard Acute Respiratory Distress  
527 Syndrome protocol, COVID-19 patients are initially put in the  
528 prone position and then put in a drug induced paralysis via a  
529 neuromuscular blockade to prevent lung injury (36). Patients  
530 are then put on a ventilator, which delivers high concentrations  
531 of oxygen while removing carbon dioxide (37). Early evidence  
532

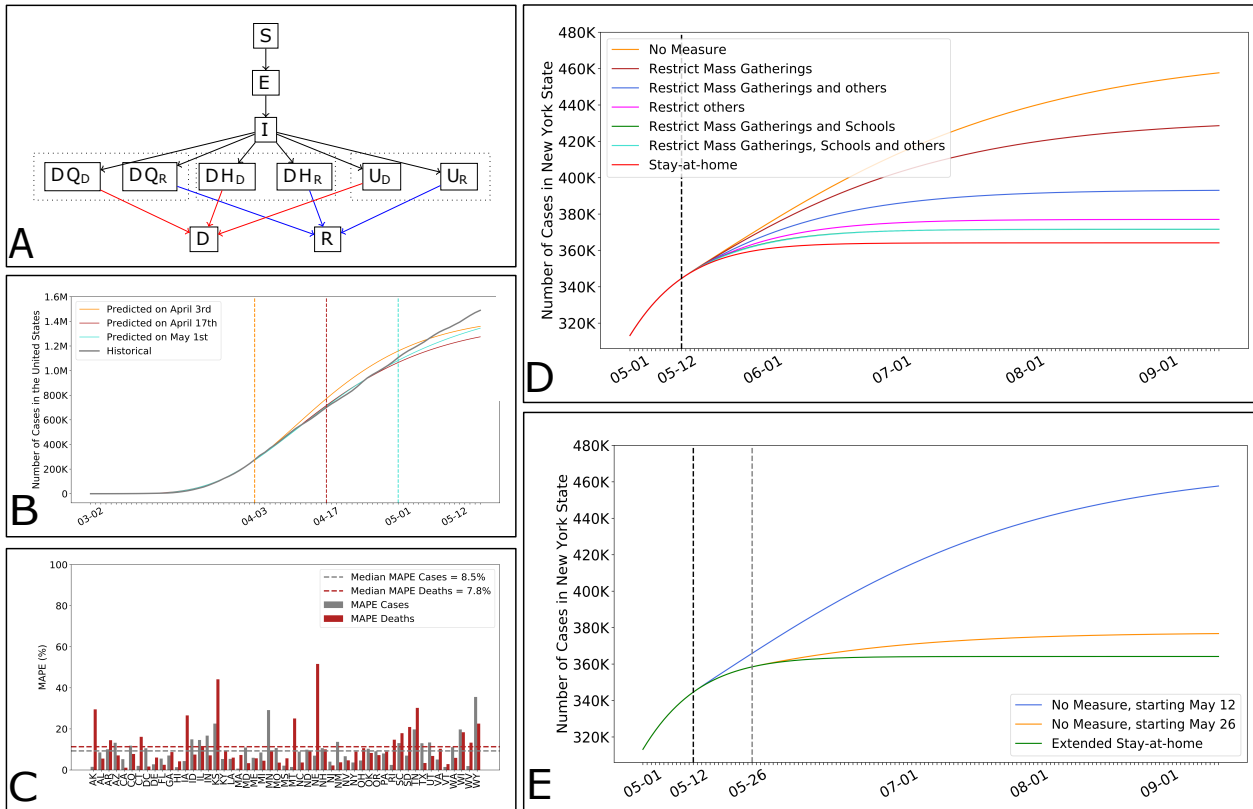


**Fig. 4.** DELPHI, an epidemiological model to guide government response. (A) Simplified flow diagram of DELPHI. (B) Cumulative number of cases in the United States according to our projections made at different points in time, against actual observations. (C) Out-of-sample Mean Absolute Percentage Error (MAPE) on the number of cases and deaths per US state. (D) Impact of different policies on the future number of cases, in NY. (E) Impact of the timing of policies on the future number of cases, in NY.

suggests that ventilator intubation reduces the risk of hypoxia for COVID-19 patients (38).

As a result, hospitals have been facing ventilator shortages worldwide (39). Still, local shortages do not necessarily imply global shortages. For instance, in April 2020, the total supply of ventilators in the United States exceeded the projected demand from COVID-19 patients. Ventilator shortages could thus be alleviated by pooling the supply, i.e., by strategically allocating the surge supply of ventilators from the federal government and facilitating inter-state transfers of ventilators.

We propose an optimization model to support the allocation of ventilators in a semi-collaborative setting where resources can be shared both between healthcare facilities or through a central authority. Based on its primary motivation, we formulate the model to support the management of the federal supply of ventilators and inter-state ventilator transfers in the United States. A similar model has also been used to support inter-hospital transfers of ventilators. The model can also support inter-country ventilator allocation during the next phases of the pandemic. This model leverages the demand projections from DELPHI-pred (Section 3) to prescribe resource allocation recommendations—with the ultimate goal of alleviating the health impact of the pandemic.

**A. Model.** Resource allocation is critical when clinical care depends on scarce equipment. Several studies have used optimization to support ventilator pooling. A time-independent model was first developed for influenza planning (40). A time-dependent stochastic optimization model was developed to sup-

port transfers to and from the federal government for COVID-19, given scenarios regarding the pandemic's spread (41). In this section, we propose a deterministic time-dependent model, leveraging the projections from DELPHI-pred.

We model ventilator pooling as a multi-period resource allocation over  $S$  states and  $D$  days. The model takes as input ventilator demand in state  $s$  and day  $d$ , denoted as  $v_{s,d}$ , as well as parameters capturing the surge supply from the federal government and the extent of inter-state collaboration. We formulate an optimization problem that decides on the number of ventilators transferred from state  $s$  to state  $s'$  on day  $d$ , and on the number of ventilators allocated from the federal government to state  $s$  on day  $d$ . We propose a bi-objective formulation. The first objective is to minimize ventilator-day shortages; for robustness, we consider both projected shortages (based on demand forecasts) and worst-case shortages (including a buffer in the demand estimates). The second objective is to minimize inter-state transfers, to limit the operational and political costs of inter-state coordination. Mixed-integer optimization provides modeling flexibility to capture spatial-temporal dynamics and the trade-offs between these various objectives. We report the mathematical formulation of the model, along with the key assumptions, in the appendix.

**B. Results.** We implemented the model on April 15, a time of pressing ventilator need in the United States. We estimate the number of hospitalizations from DELPHI-pred as the sum of  $DH_R$  and  $DH_D$ . From our clinical outcomes database in Section 1, we estimate that 25% of hospitalized patients are

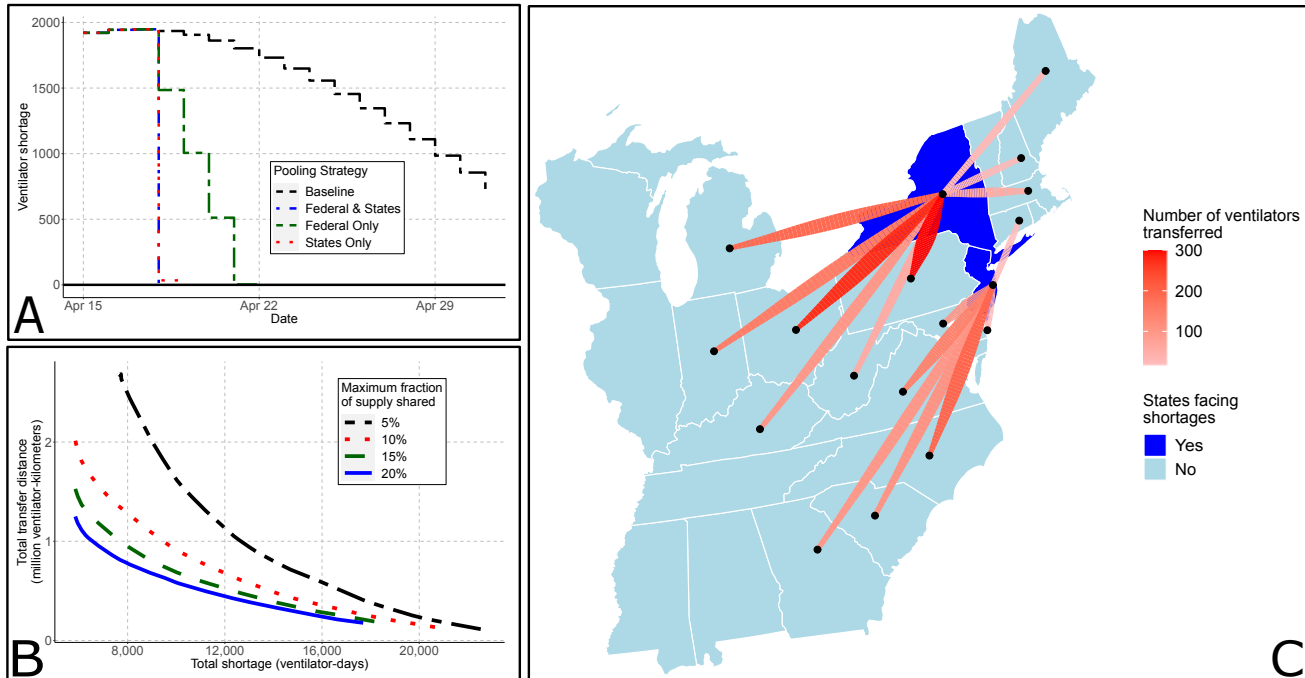


**Fig. 5.** The edge of optimization to eliminate ventilator shortages. (A) Projected shortages (in ventilator-days) in a baseline setting (without transfers) and with optimized transfers between the states and/or from the federal government. (B) Pareto frontier between transfer distance and total shortage, for different state pooling fractions. (C) Map of inter-state transfers recommended on April 15 in the US Northeast. For clarity, we do not plot shortages of fewer than 5 ventilators and transfers of fewer than 10.

put on a ventilator, which we use to estimate the demand for ventilators. We also obtain the average length of stay from our clinical outcomes database (Figure 2).

Figure 5A shows the evolution of ventilator shortages with and without ventilator transfers from the federal government and inter-state transfers. These results indicate that ventilator pooling can rapidly eliminate all ventilator shortages. Figure 5C shows ventilator transfers recommended in the US Northeast on April 15 (with inter-state transfers only), overlaid on a map displaying the predicted shortage without transfers.

There are different pathways toward eliminating ventilator shortages. Figure 5B shows the trade-off between shortages and transfer distance—each line corresponds to the maximal fraction of its own ventilators that each state can pool. Overall, states do not have to share more than 10% of their supply at any time to efficiently eliminate shortages. States can largely meet their needs with help from neighboring states, with cross-country transfers only used as a last resort. Broadly, results underscore trade-offs between ventilator shortages, the extent of inter-state transfers, the number of ventilators allocated from the federal government, and the robustness of the solution. We discuss these trade-offs further in the appendix.

**C. Discussion and Impact.** Our main insight is that ventilator shortages could be eliminated altogether through inter-state transfers and strategic management of the federal supply. Results also underscore (i) the benefits of inter-state coordination and (ii) the benefits of early coordination. First, ventilator shortages can be eliminated through inter-state transfers alone: leveraging a surge supply from the federal government is not required, though it may reduce inter-state transfers. Under our recommendation, the most pronounced transfers occur from states facing no shortages (Ohio, Pennsylvania, and North

Carolina) to states facing strong shortages (New York, New Jersey). Second, most transfers occur in early stages of the pandemic. This underscores the benefits of leveraging a predictive model like DELPHI-pred to align the ventilator supply with demand projections as early as possible.

A similar model has been developed to support the redistribution of ventilators across hospitals within the Hartford HealthCare system in Connecticut—using county-level forecasts of ventilator demand obtained from DELPHI-pred. This model has been used by a collection of hospitals in the United States to align ventilator supply with projected demand at a time where the pandemic was on the rise.

Looking ahead, the proposed model can support the allocation of critical resources in the next phases of the pandemic—spanning ventilators, medicines, personal protective equipment etc. Since epidemics do not peak in each state at the same time, states whose infection peak has already passed or lies weeks ahead can help other states facing immediate shortages at little costs to their constituents. Inter-state transfers of ventilators occurred in isolated fashion through April 2020; our model proposes an automated decision-making tool to support these decisions systematically. As our results show, proactive coordination and resource pooling can significantly reduce shortages—thus increasing the number of patients that can be treated without resorting to extreme clinical recourse with side effects (such as splitting ventilators).

## 5. Conclusion

This paper proposes a comprehensive data-driven approach to address several core challenges faced by healthcare providers and policy makers in the midst of the COVID-19 pandemic. We have gathered and aggregated data from hundreds of clin-

652 cal studies, electronic health records, and census reports. We  
653 have developed descriptive, predictive and prescriptive mod-  
654 els, combining methods from machine learning, epidemiology,  
655 and mixed-integer optimization. Results provide insights on  
656 the clinical aspects of the disease, on patients' infection and  
657 mortality risks, on the dynamics of the pandemic, and on the  
658 levers that policy makers and healthcare providers can use  
659 to alleviate its toll. The models developed in this paper also  
660 yield decision support tools that have been deployed on our  
661 dedicated website and that are actively being used by several  
662 hospitals, companies and policy makers.

## 663 Acknowledgments

664 We would like to thank Dr. Barry Stein, Dr. Ajay Kumar,  
665 Dr. Rocco Orlando, and Michelle Schneider from the Hartford  
666 HealthCare system, Dr. Angelo Pan, Dr. Rosario Canino,  
667 Sophie Testa and Federica Pezzetti from ASST Cremona, and  
668 HM Hospitals for discussions and data, as well as Hari Bandi,  
669 Katherine Bobroske, Martina Dal Bello, Vasilis Digalakis,  
670 Mohammad Fazel-Zarandi, Alvaro Fernandez Galiana, Samuel  
671 Gilmour, Adam Kim, Zhen Lin, Liangyuan Na, Matthew  
672 Sobiesk, Yuchen Wang, Sophia Xing and Cynthia Zheng from  
673 our extended team for helpful discussions.

- 674 1. G Kampf, D Todt, S Pfander, E Steinmann, Persistence of coronaviruses on inanimate sur-  
675 faces and its inactivation with biocidal agents. *J. Hosp. Infect.* (2020).
- 676 2. S Sanche1, et al., High Contagiousness and Rapid Spread of Severe Acute Respiratory  
677 Syndrome Coronavirus 2. *Emerg. Infect. Dis.* **27** (2020).
- 678 3. John Hopkins University, Center for Systems Science and Engineering  
[\(https://systems.jhu.edu/research/public/health/covid/\)](https://systems.jhu.edu/research/public/health/covid/) (2020).
- 679 4. RM Anderson, H Heesterbeek, D Klinkenberg, TD Hollingsworth, How will country-based  
680 mitigation measures influence the course of the covid-19 epidemic? *The Lancet* **395**, 931–  
681 934 (2020).
- 682 5. N Fernandes, Economic effects of coronavirus outbreak (covid-19) on the world economy.  
683 Available at SSRN 3557504 (2020).
- 684 6. WJ McKibbin, R Fernando, The global macroeconomic impacts of covid-19: Seven scenarios.  
685 *CAMA Work. Pap.* (2020).
- 686 7. US Center for Disease Control, COVID-19 Forecasts (<https://www.cdc.gov/coronavirus/2019-ncov/covid-data/forecasting-us.html>) (2020).
- 687 8. US Center for Disease Control, Symptoms of Coronavirus  
<https://www.cdc.gov/coronavirus/2019-ncov/symptoms-testing/symptoms.html> (2020)  
(Accessed 11 May 2020).
- 688 9. World Health Organization, Coronavirus (<https://www.who.int/health-topics/coronavirus>)  
(2020) (Accessed 11 May 2020).
- 689 10. National Health Service, Check if you have Coronavirus symptoms  
<https://www.nhs.uk/conditions/coronavirus-covid-19/check-if-you-have-coronavirus-symptoms> (2020) (Accessed 11 May 2020).
- 690 11. Wj Guan, et al., Clinical characteristics of coronavirus disease 2019 in china. *New Engl. journal medicine* **382**, 1708–1720 (2020).
- 691 12. P Goyal, et al., Clinical characteristics of Covid-19 in New York City. *New Engl. J. Medicine*  
(2020).
- 692 13. CM Petrelli, et al., Factors associated with hospitalization and critical illness among 4,103  
693 patients with covid-19 disease in new york city. *medRxiv* (2020).
- 694 14. P Forster, L Forster, C Renfrew, M Forster, Phylogenetic network analysis of SARS-CoV-2  
695 genomes. *Proc. Natl. Acad. Sci.* **117**, 9241–9243 (2020).
- 696 15. LA Holland, et al., An 81 nucleotide deletion in SARS-CoV-2 ORF7a identified from sentinel  
697 surveillance in Arizona (Jan-Mar 2020). *J. Virol.* (2020).
- 698 16. S Garg, Hospitalization rates and characteristics of patients hospitalized with laboratory-  
699 confirmed coronavirus disease 2019—covid-net, 14 states, march 1–30, 2020. *MMWR. Morb. Mortal. Wkly. Rep.* **69** (2020).
- 700 17. FS Vahidy, et al., Racial and ethnic disparities in sars-cov-2 pandemic: Analysis of a covid-19  
701 observational registry for a diverse us metropolitan population. *medRxiv* (2020).
- 702 18. L Lan, et al., Positive RT-PCR test results in patients recovered from COVID-19. *Jama* **323**,  
703 1502–1503 (2020).
- 704 19. O Troyanskaya, et al., Missing value estimation methods for dna microarrays. *Bioinformatics*  
705 **17**, 520–525 (2001).
- 706 20. T Chen, C Guestrin, Xgboost: A scalable tree boosting system in *Proceedings of the 22nd acm sigkdd international conference on knowledge discovery and data mining*. pp. 785–794  
707 (2016).
- 708 21. SM Lundberg, SI Lee, A unified approach to interpreting model predictions in *Advances in  
709 Neural Information Processing Systems 30*, eds. I Guyon, et al. (Curran Associates, Inc.), pp.  
710 4765–4774 (2017).
- 711 22. SM Lundberg, et al., From local explanations to global understanding with explainable AI for  
712 trees. *Nat. Mach. Intell.* **2**, 522–539 (2020).

- 723 23. Y Wang, Y Wang, Y Chen, Q Qin, Unique epidemiological and clinical features of the emerg-  
724 ing 2019 novel coronavirus pneumonia (covid-19) implicate special control measures. *J. medical virology* **92**, 568–576 (2020).  
725 24. TP Velavan, CG Meyer, The covid-19 epidemic. *Trop. medicine & international health* **25**, 278  
726 (2020).  
727 25. D Caruso, et al., Chest ct features of covid-19 in rome, italy. *Radiology*, 201237 (2020).  
728 26. C Huang, et al., Clinical features of patients infected with 2019 novel coronavirus in wuhan,  
729 china. *The Lancet* **395**, 497–506 (2020).  
730 27. W Ling, C-reactive protein levels in the early stage of COVID-19. *Med. et Maladies Infect.*  
731 (2020).  
732 28. Y Shi, et al., COVID-19 infection: the perspectives on immune responses (2020).  
733 29. Q Shi, et al., Serum calcium as a biomarker of clinical severity and prognosis in patients with  
734 coronavirus disease 2019: a retrospective cross-sectional study. (2020).  
735 30. RE Jordan, P Adab, K Cheng, Covid-19: risk factors for severe disease and death (2020).  
736 31. Y Liu, et al., Neutrophil-to-lymphocyte ratio as an independent risk factor for mortality in  
737 hospitalized patients with covid-19. *J. Infect.* (2020).  
738 32. F Zhou, et al., Clinical course and risk factors for mortality of adult inpatients with covid-19 in  
739 wuhan, china: a retrospective cohort study. *The Lancet* (2020).  
740 33. SM Kissler, C Tedijanti, E Goldstein, YH Grad, M Lipsitch, Projecting the transmission dy-  
741 namics of sars-cov-2 through the postpandemic period. *Science* (2020).  
742 34. New York Times, Coronavirus in the U.S.: Latest Map and Case Count  
<https://www.nytimes.com/interactive/2020/us/coronavirus-us-cases.html> (2020).  
743 35. L Breiman, J Friedman, CJ Stone, RA Olshen, *Classification and regression trees*. (CRC  
744 press), (1984).  
745 36. RA Cornejo, et al., Effects of prone positioning on lung protection in patients with acute  
746 respiratory distress syndrome. *Am. journal respiratory critical care medicine* **188**, 440–448  
747 (2013).  
748 37. T Bein, et al., The standard of care of patients with ARDS: ventilatory settings and rescue  
749 therapies for refractory hypoxemia. *Intensive care medicine* **42**, 699–711 (2016).  
750 38. L Meng, et al., Intubation and Ventilation amid the COVID-19 OutbreakWuhan's Experience.  
751 *Anesthesiol. The J. Am. Soc. Anesthesiol.* (2020).  
752 39. ML Ranney, V Griffith, AK Jha, Critical supply shortages—the need for ventilators and per-  
753 sonal protective equipment during the Covid-19 pandemic. *New Engl. J. Medicine* (2020).  
754 40. HC Huang, et al., Stockpiling ventilators for influenza pandemics. *Emerg. infectious diseases*  
755 **23**, 914 (2017).  
756 41. S Mehrotra, H Rahimian, M Barah, F Luo, K Schantz, A model of supply-chain decisions for  
757 resource sharing with an application to ventilator allocation to combat COVID-19. *Nav. Res.  
758 Logist. (NRL)* (2020).  
759 42. S Mehrotra, H Rahimian, M Barah, F Luo, K Schantz, A model of supply-chain decisions for  
760 resource sharing with an application to ventilator allocation to combat COVID-19. *Nav. Res.  
761 Logist. (NRL)* (2020).